Constraining the Higgs-gauge couplings through differential SMEFT analyses

Shankha Banerjee
IPPP, Durham University
LHCP 2020

May 29, 2020

Based on

Phys. Rev. D 98, 095012 (2018), arXiv:1807.01796 (with R. S. Gupta, C. Englert and M. Spannowsky)

Phys. Rev. D 100, 115004, arXiv:1905.02728 (with R. S. Gupta, J. Y. Reiness and M. Spannowsky)

arXiv: 1912.07628 (with R. S. Gupta, J. Y. Reiness, S. Seth and M. Spannowsky)

arXiv: 2006.abcde (with J. Y. Araz, R. S. Gupta and M. Spannowsky)

SMEFT Motivation

- Q: How do we reconstruct a TeV-Scale Lagrangian from this data?
- Q: How to extract the best observables to study the effects of a particular operator and for a particular process?
- New vertices ensuing from EFT can produce novel/ enhanced effects in parts of the phase space
- These questions and ideas can be addressed in the regime of high energies/ luminosities

- A bigger theory (either weakly or strongly coupled) is assumed to supersede the SM above the scale Λ
- At the perturbative level, all heavy ($> \Lambda$) DOF are decoupled from the low energy theory (Appelquist-Carazzone theorem)
- Appearance of HD operators in the effective Lagrangian valid below Λ

$$\mathcal{L} = \mathcal{L}_{SM}^{d=4} + \sum_{d\geq 5} \sum_{i} \frac{f_i}{\Lambda^{d-4}} \mathcal{O}_i^d$$

- Precisely measuring the Higgs couplings $\longrightarrow$ one of the most important LHC goals
- Indirect constraints can constrain much higher scales S, T parameters being prime examples
- Q: Can LHC compete with LEP in constraining precision physics? Can LHC provide new information?
A: From EFT correlated variables, LEP already constrained certain anomalous Higgs couplings $\longrightarrow$ Z-pole measurements, TGCs
Going to higher energies in LHC is the only way to obtain new information

Case study I: Higgs-Strahlung at the LHC

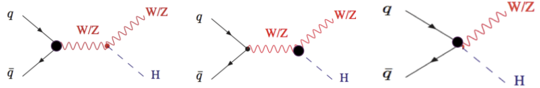

$$
\begin{aligned}
\Delta\mathcal{L}_6 \quad \supset \quad & \delta\hat{g}^h_{WW}\,\frac{2m_W^2}{v}hW^{+\mu}W^-_\mu + \delta\hat{g}^h_{ZZ}\,\frac{2m_Z^2}{v}h\frac{Z^\mu Z_\mu}{2} + \delta g^W_Q\,(W^+_\mu\bar{u}_L\gamma^\mu d_L + h.c.) \\
+ \quad & \delta g^W_L\,(W^+_\mu\bar{\nu}_L\gamma^\mu e_L + h.c.) + g^h_{WL}\,\frac{h}{v}(W^+_\mu\bar{\nu}_L\gamma^\mu e_L + h.c.) \\
+ \quad & g^h_{WQ}\,\frac{h}{v}(W^+_\mu\bar{u}_L\gamma^\mu d_L + h.c.) + \sum_f \delta g^Z_f Z_\mu\bar{f}\gamma^\mu f + \sum_f g^h_{Zf}\,\frac{h}{v}Z_\mu\bar{f}\gamma^\mu f \\
+ \quad & \kappa_{WW}\,\frac{h}{v}W^{+\mu\nu}W^-_{\mu\nu} + \tilde{\kappa}_{WW}\,\frac{h}{v}W^{+\mu\nu}\tilde{W}^-_{\mu\nu} + \kappa_{ZZ}\,\frac{h}{2v}Z^{\mu\nu}Z_{\mu\nu} \\
+ \quad & \tilde{\kappa}_{ZZ}\,\frac{h}{2v}Z^{\mu\nu}\tilde{Z}_{\mu\nu} + \kappa_{Z\gamma}\,\frac{h}{v}A^{\mu\nu}Z_{\mu\nu} + \tilde{\kappa}_{Z\gamma}\,\frac{h}{v}A^{\mu\nu}\tilde{Z}_{\mu\nu} + \delta\hat{g}^h_{bb}\,\frac{\sqrt{2}m_b}{v}hb\bar{b}
\end{aligned}
$$

- The leading effect comes from contact interaction at high energies. The energy growth occurs because there is no propagator
- δg^Z_f, $\delta\hat{g}^h_{ZZ}$ (and other terms in blue) $\rightarrow$ deviations in SM amplitude
- These do not grow with energy and are suppressed by $\mathcal{O}(m_Z^2/\hat{s})$ w.r.t. g^h_{Vf}

Higgs-Strahlung: Operators at play

$\mathcal{O}_{H\Box} = (H^\dagger H)\Box(H^\dagger H)$	$\mathcal{O}_{HL}^{(3)} = iH^\dagger\sigma^a \overleftrightarrow{D}_\mu H\bar{L}\sigma^a\gamma^\mu L$
$\mathcal{O}_{HD} = (H^\dagger D_\mu H)^*(H^\dagger D_\mu H)$	$\mathcal{O}_{HB} = \lvert H\rvert^2 B_{\mu\nu}B^{\mu\nu}$
$\mathcal{O}_{Hu} = iH^\dagger \overleftrightarrow{D}_\mu H\bar{u}_R\gamma^\mu u_R$	$\mathcal{O}_{HWB} = H^\dagger\sigma^a H W^a_{\mu\nu}B^{\mu\nu}$
$\mathcal{O}_{Hd} = iH^\dagger \overleftrightarrow{D}_\mu H\bar{d}_R\gamma^\mu d_R$	$\mathcal{O}_{HW} = \lvert H\rvert^2 W_{\mu\nu}W^{\mu\nu}$
$\mathcal{O}_{He} = iH^\dagger \overleftrightarrow{D}_\mu H\bar{e}_R\gamma^\mu e_R$	$\mathcal{O}_{H\tilde{B}} = \lvert H\rvert^2 B_{\mu\nu}\tilde{B}^{\mu\nu}$
$\mathcal{O}_{HQ}^{(1)} = iH^\dagger \overleftrightarrow{D}_\mu H\bar{Q}\gamma^\mu Q$	$\mathcal{O}_{H\tilde{W}B} = H^\dagger\sigma^a H W^a_{\mu\nu}\tilde{B}^{\mu\nu}$
$\mathcal{O}_{HQ}^{(3)} = iH^\dagger\sigma^a \overleftrightarrow{D}_\mu H\bar{Q}\sigma^a\gamma^\mu Q$	$\mathcal{O}_{H\tilde{W}} = \lvert H\rvert^2 W^a_{\mu\nu}\tilde{W}^{a\mu\nu}$
$\mathcal{O}_{HL}^{(1)} = iH^\dagger \overleftrightarrow{D}_\mu H\bar{L}\gamma^\mu L$	$\mathcal{O}_{y_b} = y_b\lvert H\rvert^2(\bar{Q}Hb_R + h.c).$

Table: D6 operators in Warsaw basis contributing to anomalous $hVV^*/hV\bar{f}f$ couplings.

Differential in energy and angles: $pp \to V(\ell\ell)h$ (Fat jet)

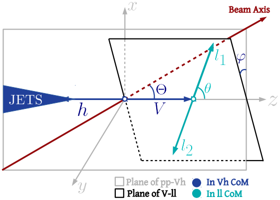

- φ, Θ and $\{x, y, z\}$ in Vh CoM frame (z identified as direction of V-boson; y identified as normal to the plane of V and beam axis; x defined to complete the right-handed set), θ in V CoM frame
- Q: How much differential information can one extract from this process?
- For three body phase space, $3 \times 3 - 4 = 5$ kinematic variables completely define final state
- Barring boost factor, the variables are $\sqrt{s}, \Theta, \theta, \varphi$
- Considering 10 bins per variable $\to$ 1000 numbers per energy bin to obtain full information $\to$ can be reduced to 9 per energy bin

Differential in Energy: $pp \to Zh$ at high energies (Contact term)

- The differential cross-section for the processes $pp \to Z(\ell^+\ell^-)/W(\ell\nu)h(b\bar{b})$ is a differential in four variables, *viz.*, $\frac{d\sigma}{dEd\Theta d\theta d\varphi}$
- Major background $Zb\bar{b}$ (b-tagging efficiency taken to be 70%)
- Boosted substructure analysis with fat-jets of $R = 1.2$ used
- $\sigma_{Zh}^{SM}/\sigma_{Zb\bar{b}}$ without cuts $\sim 4.6/165$; With the cut-based analysis $\to 0.26$
- With MVA optimisation $\to 0.50$ See also [Freitas, Khosa and Sanz, 2019]
- S/B changes from $1/40$ to $\mathcal{O}(1)$ $\to$ Close to 35 SM $Zh(b\bar{b}\ell^+\ell^-)$ events left at 300 fb^{-1}

  [SB, Englert, Gupta, Spannowsky, 2018]; NLO corrections: [Greljo, Isidori, Lindert, Marzocca, Zhang, 2017]

- See Nan Lu's slides for possible updates using future detector upgrades

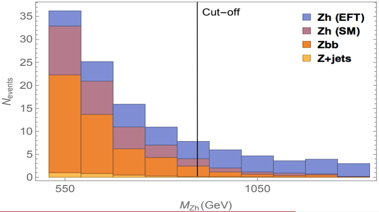

Cuts	Zbb	Zh (SM)
At least 1 fat jet with 2 B-mesons with $p_T > 15$ GeV	0.23	0.41
2 OSSF isolated leptons	0.41	0.50
80 GeV $< M_{\ell\ell} <$ 100 GeV, $p_{T,\ell\ell} > 160$ GeV, $\Delta R_{\ell\ell} > 0.2$	0.83	0.89
At least 1 fat jet with 2 B-meson tracks with $p_T > 110$ GeV	0.96	0.98
2 Mass drop subjets and ≥ 2 filtered subjets	0.88	0.92
2 b-tagged subjets	0.38	0.41
115 GeV $< m_h <$ 135 GeV	0.15	0.51
$\Delta R(b_i, \ell_j) > 0.4$, $\not{E}_T < 30$ GeV, $\lvert y_h \rvert < 2.5$, $p_{T,h/Z} > 200$ GeV	0.47	0.69

Differential in Energy: $pp \to Zh$ at high energies (Contact term)

- Two-parameter χ^2-fit (at 300 fb^{-1}) in $\delta g_1^Z - (\delta\kappa_\gamma - \hat{S})$ plane

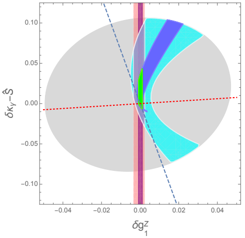

Blue dashed line $\longrightarrow$ direction of accidental cancellation of interference term; Gray region: LEP exclusion; pink band: exclusion from *WZ* [Franceschini, Panico, Pomarol, Riva and Wulzer, 2017]; Blue region: exclusion from *Zh*; dark (light) shade represents bounds at 3 ab^{-1} (300 fb^{-1}) luminosity; Green region: Combined bound from *Zh* and *WZ* [SB, Englert, Gupta, Spannowsky, 2018]

- Bounds on pseudo observables
- Our bounds are derived by considering one parameter at a time and upon considering only interference (at 95% CL). The four directions in LEP are at 68% CL.

$$g^Z_{\mathbf{p}} = g^h_{Zu_L} - 0.76\ g^h_{Zd_L} - 0.45\ g^h_{Zu_R} + 0.14\ g^h_{Zd_R}$$

$$g^h_{Z\mathbf{p}} \in [-0.004, 0.004] \qquad (300\ \text{fb}^{-1})$$
$$g^h_{Z\mathbf{p}} \in [-0.001, 0.001] \qquad (3000\ \text{fb}^{-1})$$

	Our Projection	LEP Bound
$\delta g^Z_{u_L}$	±0.002 (±0.0007)	-0.0026 ± 0.0016
$\delta g^Z_{d_L}$	±0.003 (±0.001)	0.0023 ± 0.001
$\delta g^Z_{u_R}$	±0.005 (±0.001)	-0.0036 ± 0.0035
$\delta g^Z_{d_R}$	±0.016 (±0.005)	0.016 ± 0.0052
δg^Z_1	±0.005 (±0.001)	$0.009^{+0.043}_{-0.042}$
$\delta\kappa_\gamma$	±0.032 (±0.009)	$0.016^{+0.085}_{-0.096}$
$\hat{S}$	±0.032 (±0.009)	0.0004 ± 0.0007
W	±0.003 (±0.001)	0.0000 ± 0.0006
Y	±0.032 (±0.009)	0.0003 ± 0.0006

Helicity Amplitudes

- For a $2 \to 2$ process $f(\sigma)\bar{f}(-\sigma) \to Vh$, the helicity amplitudes are given by

$$\mathcal{M}_{\sigma}^{\lambda=\pm} = \sigma \frac{1+\sigma\lambda\cos\Theta}{\sqrt{2}} G_V \frac{m_V}{\sqrt{\hat{s}}} \left[1 + \left(\frac{g^h_{Vf}}{g^V_f} + \hat{\kappa}_{VV} - i\lambda\hat{\tilde{\kappa}}_{VV}\right)\frac{\hat{s}}{2m_V^2}\right]$$

$$\mathcal{M}_{\sigma}^{\lambda=0} = -\frac{\sin\Theta}{2} G_V \left[1 + \delta\hat{g}^h_{VV} + 2\hat{\kappa}_{VV} + \delta g^Z_f + \frac{g^h_{Vf}}{g^V_f}\left(-\frac{1}{2} + \frac{\hat{s}}{2m_V^2}\right)\right]$$

$$[\hat{\kappa}_{WW} = \kappa_{WW}, \hat{\kappa}_{ZZ} = \kappa_{ZZ} + \frac{Q_f e}{g^Z_f}\kappa_{Z\gamma}, \hat{\tilde{\kappa}}_{ZZ} = \tilde{\kappa}_{ZZ} + \frac{Q_f e}{g^Z_f}\tilde{\kappa}_{Z\gamma}]$$

- $\lambda = \pm 1$ and $\sigma = \pm 1$ are, respectively, the helicities of the Z/W-boson and initial-state fermions, $g^Z_f = g(T^f_3 - Q_f s^2_{\theta_W})/c_{\theta_W}$
- Leading SM is longitudinal ($\lambda = 0$), Leading effect of κ_{WW}, $\kappa_{ZZ}, \tilde{\kappa}_{ZZ}$ is in the transverse-longitudinal (LT) interference, LT term vanishes if we aren't careful
- The amplitude at decay level: $\mathcal{A}(\hat{s},\Theta,\theta,\varphi) = \frac{-ig^V_\ell + \delta g^V_\ell}{\Gamma_V}\sum_\lambda \mathcal{M}^\lambda_\sigma(\hat{s},\Theta) d^{J=1}_{\lambda,1}(\theta) e^{i\lambda\hat{\varphi}}$
- $d^{J=1}_{\pm 1,1} = \tau\frac{1\pm\tau\cos\theta}{\sqrt{2}}$, $d^{J=1}_{0,1} = \sin\theta$ are the Wigner functions, τ is lepton helicity, Γ_V is the V-width and $g^Z_f = g(T^f_3 - Q_f s^2_{\theta_W})/c_{\theta_W}$ and $g^W_f = g/\sqrt{2}$
- $\hat{\varphi} \to$ azimuthal angle of positive helicity lepton, $\hat{\theta} \to$ its polar angle in V-rest frame
- Polarisation of lepton is experimentally not accessible

Helicity Amplitudes: Angular Moments

- We sum over lepton polarisations and express the analogous angles (θ, φ) for the positively-charged lepton

$$\sum_{L,R} |\mathcal{A}(\hat{s}, \Theta, \theta, \varphi)|^2 \quad = \quad \alpha_L |\mathcal{A}_h(\hat{s}, \Theta, \theta, \varphi)|^2 + \alpha_R |\mathcal{A}_h(\hat{s}, \Theta, \pi - \theta, \pi + \varphi)|^2$$

- $\alpha_{L,R} = (g^Z_{l_{L,R}})^2 / [(g^Z_{l_L})^2 + (g^Z_{l_R})^2] \rightarrow$ fraction of $Z \rightarrow \ell^+\ell^-$ decays to leptons with left-handed (right-handed) chiralities $\epsilon_{LR} = \alpha_L - \alpha_R \approx 0.16$
- For left-handed chiralities, positive-helicity lepton $\rightarrow$ positive-charged lepton
- For right-handed chiralities, positive-helicity lepton $\rightarrow$ negative-charged lepton $\rightarrow$ $(\hat{\theta}, \hat{\varphi}) \rightarrow (\pi - \theta, \pi + \varphi) \rightarrow$ Following 9 coefficients are 9 angular moments for $pp \rightarrow Z(\ell\ell)h$

$$\begin{aligned}
\sum_{L,R} |\mathcal{A}(\hat{s}, \Theta, \theta, \varphi)|^2 &= a_{LL} \sin^2\Theta \sin^2\theta + a^1_{TT} \cos\Theta \cos\theta \\
&+ a^2_{TT}(1 + \cos^2\Theta)(1 + \cos^2\theta) + \cos\varphi \sin\Theta \sin\theta \\
&\times (a^1_{LT} + a^2_{LT} \cos\theta \cos\Theta) + \sin\varphi \sin\Theta \sin\theta \\
&\times (\tilde{a}^1_{LT} + \tilde{a}^2_{LT} \cos\theta \cos\Theta) + a_{TT'} \cos 2\varphi \sin^2\Theta \sin^2\theta \\
&+ \tilde{a}_{TT'} \sin 2\varphi \sin^2\Theta \sin^2\theta
\end{aligned}$$

See also [Azatov, Elias-Miro, Reyimuaji, Venturini; 2017]

Differential in angles: Constraining the LT terms

a_{LL}	$\frac{\mathcal{G}^2}{4}\left[1+2\delta\hat{g}^h_{VV}+4\hat{\kappa}_{VV}+2\delta g^Z_f+\frac{g^h_{Vf}}{g^V_f}(-1+4\gamma^2)\right]$
a^1_{TT}	$\frac{\mathcal{G}^2\sigma\epsilon_{RL}}{2\gamma^2}\left[1+4\left(\frac{g^h_{Vf}}{g^V_f}+\hat{\kappa}_{VV}\right)\gamma^2\right]$
a^2_{TT}	$\frac{\mathcal{G}^2}{8\gamma^2}\left[1+4\left(\frac{g^h_{Vf}}{g^V_f}+\hat{\kappa}_{VV}\right)\gamma^2\right]$
a^1_{LT}	$-\frac{\mathcal{G}^2\sigma\epsilon_{RL}}{2\gamma}\left[1+2\left(\frac{2g^h_{Vf}}{g^V_f}+\hat{\kappa}_{VV}\right)\gamma^2\right]$
a^2_{LT}	$-\frac{\mathcal{G}^2}{2\gamma}\left[1+2\left(\frac{2g^h_{Vf}}{g^V_f}+\hat{\kappa}_{VV}\right)\gamma^2\right]$
$\tilde{a}^1_{LT}$	$-\mathcal{G}^2\sigma\epsilon_{RL}\hat{\tilde{\kappa}}_{VV}\gamma$
$\tilde{a}^2_{LT}$	$-\mathcal{G}^2\hat{\tilde{\kappa}}_{VV}\gamma$
$a_{TT'}$	$\frac{\mathcal{G}^2}{8\gamma^2}\left[1+4\left(\frac{g^h_{Vf}}{g^V_f}+\kappa_{\hat{V}V}\right)\gamma^2\right]$
$\tilde{a}_{TT'}$	$\frac{\mathcal{G}^2}{2}\hat{\tilde{\kappa}}_{VV}$

Contribution of the different anomalous couplings to the angular coefficients up to linear order. Contributions subdominant in $\gamma = \sqrt{\hat{s}}/(2m_V)$ are neglected, with the exception of the next-to-leading EFT contribution to a_{LL}, which we retain in order to keep the leading effect of the $\delta\hat{g}^h_{VV}$ term. $\mathcal{G} = gg^Z_f\sqrt{(g^Z_{l_L})^2+(g^Z_{l_R})^2}/(c_{\theta_W}\Gamma_Z)$.

- As anticipated, the parametrically-largest contribution is to the LT interference terms

$$\frac{a^2_{LT}}{4}\cos\varphi\sin 2\theta\sin 2\Theta + \frac{\tilde{a}^2_{LT}}{4}\sin\varphi\sin 2\theta\sin 2\Theta$$

- These terms vanish on integration of any angle
- Q: How to probe κ_{ZZ} and $\tilde{\kappa}_{ZZ}$?
  A: Simplified approach $\longrightarrow$ Flip sign in regions to maintain positive $\sin 2\theta\sin 2\Theta$
  A: Sophisticated approach $\longrightarrow$ Use method of moments
- Expect $\cos\varphi$ distribution for CP-even and $\sin\varphi$ distribution for CP-odd

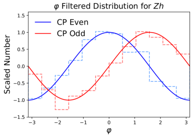

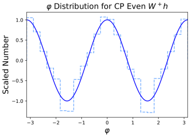

Q: Are the LO theoretical shapes preserved upon the inclusion of NLO effects, radiations, showering, experimental cuts, etc.?
A: For the azimuthal angles, they are. [SB, Gupta, Reiness, Spannowsky; 2019], [SB, Gupta, Reiness, Seth, Spannowsky; 2019]

Differential in angles: Method of moments

- An analog of Fourier analysis utilised to extract the aforementioned angular moments
- Our squared amplitude can be parametrised as, $|\mathcal{A}|^2 = \sum_i a_i(E) f_i(\Theta, \theta, \varphi)$
- We look for weight functions, $w_i(\Theta, \theta, \varphi)$, such that $< w_i | f_i >= \int d(\Theta, \theta, \varphi) w_i f_j = \delta_{ij}$
- One can then pick out the angular moments, a_i as $a_i = \int d(\Theta, \theta, \varphi) |\mathcal{A}|^2 w_i$

- For the set of basis functions, we get the following matrix

$$M = \begin{pmatrix} \frac{512\pi}{225} & 0 & \frac{128\pi}{25} & 0 & 0 & 0 & 0 & 0 & 0 \\ 0 & \frac{8\pi}{9} & 0 & 0 & 0 & 0 & 0 & 0 & 0 \\ \frac{128\pi}{25} & 0 & \frac{6272\pi}{225} & 0 & 0 & 0 & 0 & 0 & 0 \\ 0 & 0 & 0 & \frac{16\pi}{9} & 0 & 0 & 0 & 0 & 0 \\ 0 & 0 & 0 & 0 & \frac{16\pi}{225} & 0 & 0 & 0 & 0 \\ 0 & 0 & 0 & 0 & 0 & \frac{16\pi}{9} & 0 & 0 & 0 \\ 0 & 0 & 0 & 0 & 0 & 0 & \frac{16\pi}{225} & 0 & 0 \\ 0 & 0 & 0 & 0 & 0 & 0 & 0 & \frac{256\pi}{225} & 0 \\ 0 & 0 & 0 & 0 & 0 & 0 & 0 & 0 & \frac{256\pi}{225} \end{pmatrix}$$

- $w_i \propto f_i$ except for $i = 1, 3$
- We rotate the (1,3) system to an orthogonal basis
- Using discrete method, we find: $a_i(M) = \frac{\hat{N}}{N} \sum_{n=1}^{N} w_i(\Theta_n, \theta_n, \varphi_n)$
- Events divided in bins of final state invariant mass ($M \to$ central value of bin), $N(M)(N(\hat{M})) \to$ number of MC (actual) events in that bin for a fixed integrated luminosity

Results: Contact terms, Zh, Wh, $Zh + Wh$ combination

- We have limited our calculations to include only the interference terms
- The four-point contact vertex is constrained upon using the E^2 dependent terms
- The a_{LL} term dominates at high energies $\rightarrow |g^h_{WQ}| < 6 \times 10^{-4}$ and $\rightarrow |g^h_{Zf}| < 4 \times 10^{-4}$ at $\mathcal{L} = 3$ ab^{-1}

- Method of moments used to constrain the other couplings
- We obtain percent level bounds on κ_{ZZ} and in the $(\kappa_{ZZ}, \delta\hat{g}^h_{ZZ})$ plane
- Competitive and complementary bounds to previous analyses
- Independent bound on the CP-odd coupling, $|\tilde{\kappa}^{\mathbf{p}}_{ZZ}| < 0.03$

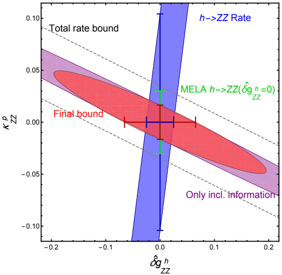

- We obtain percent level bounds on κ_{WW} and in the $(\kappa_{WW}, \delta\hat{g}^h_{WW})$ plane
- Competitive and complementary bounds to previous analyses
- Independent bound on the CP-odd coupling, $|\tilde{\kappa}^{\mathbf{p}}_{WW}| < 0.04$

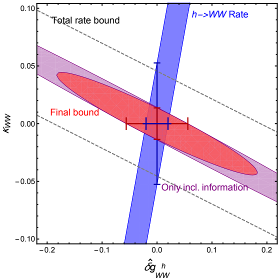

- Upon assuming a linearly realised electroweak symmetry and correlations, we can combine the above bounds

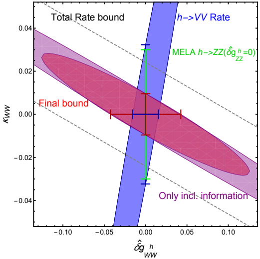

Case study II: Weak boson fusion (preliminary)

- Process: $pp \to h(\gamma\gamma)jj$
- Fake backgrounds are still to be taken properly
- $h \to \tau\tau$ analyses are underway

	Background		SM Signal	
	Events	Efficiency	Events	Efficiency
Presel.	369176.1 (3691761.0)	-	1365.2 (13651.6)	-
Njet≥ 2	286704.2 (2867042.3)	77.66%	1144.9 (11449.3)	83.87%
Bjet veto	274869.6 (2748696.5)	95.87%	1108.2 (11081.7)	96.79%
$\lvert\Delta\eta_{jj}\rvert > 3$	164813.0 (1648129.7)	59.96%	838.0 (8380.1)	75.62%
$\eta_{j_1}\cdot\eta_{j_2} < 0$	161844.1 (1618441.5)	98.20%	827.2 (8272.2)	98.71%
$M_{jj} > 600$ [GeV]	93105.4 (931054.2)	57.53%	658.6 (6586.0)	79.62%
$N_\gamma = 2$	20244.1 (202441.2)	21.74%	432.8 (4328.5)	65.72%
$I_\gamma^{rel} < 15\%$	19876.9 (198768.7)	98.19%	431.9 (4318.6)	99.77%
$\Delta R_{\gamma j}^{min} > 1.5$	8379.1 (83790.7)	42.15%	382.6 (3825.6)	88.58%
$\lvert\Delta\Phi_{\gamma\gamma,jj}\rvert > 1.5$	7896.7 (78967.4)	94.24%	373.4 (3734.4)	97.62%
$\Delta\Phi_{j_1,j_2} < 2$	2393.7 (23936.9)	30.31%	227.7 (2277.0)	60.97%
$122 < M_{\gamma\gamma} < 128$ [GeV]	88.1 (880.6)	3.68%	226.9 (2268.9)	99.64%
$y_{j_{1,2}}^{min} < y_h < y_{j_{1,2}}^{max}$	78.0 (780.4)	88.63%	223.2 (2232.5)	98.40%
S/B	286.06%			
S/(B+S)	74.10%			
$S/\sqrt{B}$	25.27 (79.91)			

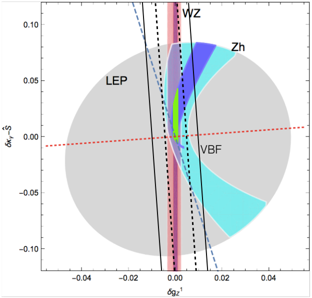

Direction: $g_{\mathbf{p}}^{VBF} = g_{Zu_L}^h - 0.93 g_{Zd_L}^h - 0.13 g_{Zu_R}^h + 0.04 g_{Zd_R}^h$

[J. Y. Araz, SB, R. S. Gupta, M. Spannowsky, *Coming soon!!!*]

STXS (plots from LHC Higgs cross-section WG's note)

- Evolving from signal strength measurements performed during Run I, by reducing uncertainties and by providing finely-grained measurements
- Allows combination of measurements in several decay channels. Several stages proposed. Measuring cross-sections instead of signal strengths
- Stage 0 corresponds to production mode categorisation; Stage 1 defines complete setup with potential bin merging etc.
- From the various bins, one can translate to signal strength measurements, measurements on EFT coefficients, BSM coefficients etc.

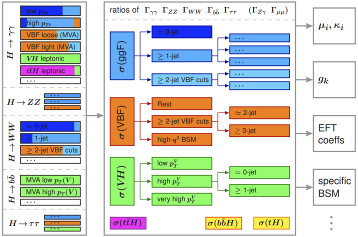

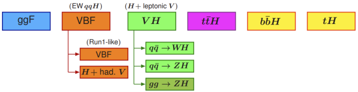

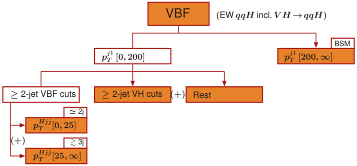

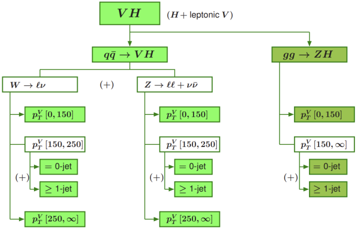

STXS (slide from S. Jiggins)

VH→ bb STXS

ATLAS-CONF-2020-006
ATLAS-CONF-2020-007

→ **VHbb resolved:** Stage 1.2 STXS scheme merged down to 5 bins

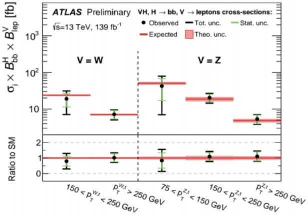

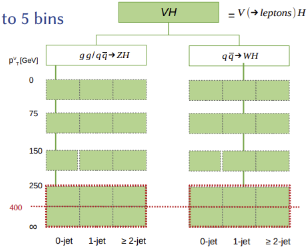

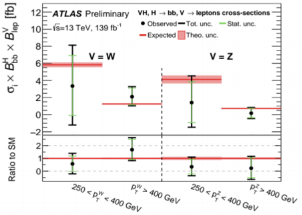

→ **VHbb Resolved:** Increased precision of 5 POI $\sigma^{W/ZH}$ results:

80fb^{-1}: 50%-125% uncertainty on $\sigma^{W/ZH}$

139fb^{-1}: 30%-85% uncertainty on $\sigma^{W/ZH}$

→ **VHbb boosted:** Stage 1.2 STXS scheme merged down to **4 bins**

- Measurement of p^V_T(truth) > 400 GeV

→ VHbb resolved + boosted **not orthogonal!**

→ See talk by Nikita Belyaev for more STXS/EFT results

→ Or backup for questions!

Stephen Jiggins 10

See slides from Stephen Jiggins, Jonathan M. Langford and Nikita Belyaev

STXS (plots from J. M. Langford)

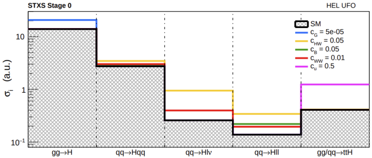

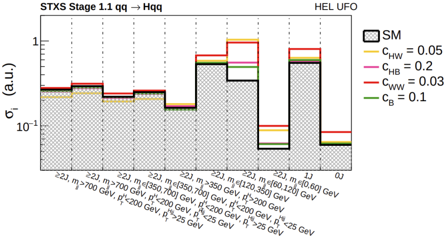

- The STXS method evolves with increasing statistics and requires intuition and systematic understanding of the data
- The various stages of binning help us with an excellent understanding of the present data
- STXS gradually moves forward to a fully differential analysis with shape information
- STXS can be connected to EFTs, κ framework, various BSM scenarios, etc. It is a powerful tool.
- The Matrix Element Method (MEM) is one of the most powerful tools to discern the full structure of any process
- The Method of Moments (MoM), as described in this talk, has comparable sensitivity to the Matrix Element method
- MoM exploits the full angular structure for the squared amplitude in a transparent and experiment-friendly manner
- MoM combines the advantages of both STXS and the MEM, to a certain extent

Summary and conclusions

- HL-LHC can thus strongly compete with LEP and can be considered a good precision machine at the moment
- EFT's essence shows that many anomalous Higgs couplings were already constrained by LEP through Z-pole and di-boson measurements
- The full hZZ and hWW tensor structures can be disentangled by using fully differential information and sophisticated techniques like the Method of moments
- Studying complementary directions like the WBF is also important
- STXS is a powerful tool that gains in sophistication with more data accumulated
- One should explore the STXS, MoM and Matrix Element methods for comparison and transparency
- Upcoming work using the MoM method for the $gg \to h \to ZZ^* \to 4\ell$ channel [SB, R. S. Gupta, M. Spannowsky, O. Ochoa-Valeriano and E. Venturini] $\to$ Stay tuned!!!

For further questions, please join: [Zoom link]

Meeting ID: 925 6370 6395, Password: 596513

Backup Slides

STU oblique parameters

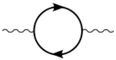

$$\Pi_{\gamma\gamma}(q^2) = q^2\Pi'_{\gamma\gamma}(0)+\dots$$
$$\Pi_{Z\gamma}(q^2) = q^2\Pi'_{Z\gamma}(0)+\dots$$
$$\Pi_{ZZ}(q^2) = \Pi_{ZZ}(0) + q^2\Pi'_{ZZ}(0)+\dots$$
$$\Pi_{WW}(q^2) = \Pi_{WW}(0) + q^2\Pi'_{WW}(0)+\dots$$

$$\alpha S = 4s_w^2c_w^2\left[\Pi'_{ZZ}(0) - \frac{c_w^2 - s_w^2}{s_w c_w}\Pi'_{Z\gamma}(0) - \Pi'_{\gamma\gamma}(0)\right]$$
$$\alpha T = \frac{\Pi_{WW}(0)}{M_W^2} - \frac{\Pi_{ZZ}(0)}{M_Z^2}$$
$$\alpha U = 4s_w^2\left[\Pi'_{WW}(0) - c_w^2\Pi'_{ZZ}(0) - 2s_wc_w\Pi'_{Z\gamma}(0) - s_w^2\Pi'_{\gamma\gamma}(0)\right]$$

1. Any BSM correction which is indistinguishable from a redefinition of e, G_F and M_Z (or equivalently, g_1, g_2 and v) in the Standard Model proper at the tree level does not contribute to S, T or U.
2. Assuming that the Higgs sector consists of electroweak doublet(s) H, the effective action term $\left|H^\dagger D_\mu H\right|^2/\Lambda^2$ only contributes to T and not to S or U. This term violates custodial symmetry.
3. Assuming that the Higgs sector consists of electroweak doublet(s) H, the effective action term $H^\dagger W^{\mu\nu}B_{\mu\nu}H/\Lambda^2$ only contributes to S and not to T or U. (The contribution of $H^\dagger B^{\mu\nu}B_{\mu\nu}H/\Lambda^2$ can be absorbed into g_1 and the contribution of $H^\dagger W^{\mu\nu}W_{\mu\nu}H/\Lambda^2$ can be absorbed into g_2).
4. Assuming that the Higgs sector consists of electroweak doublet(s) H, the effective action term $\left(H^\dagger W^{\mu\nu}H\right)\left(H^\dagger W_{\mu\nu}H\right)/\Lambda^4$ contributes to U.

VH: Relations to the Warsaw Basis

$$
\begin{aligned}
g^h_{Wf} &= \sqrt{2}g\frac{v^2}{\Lambda^2}c^{(3)}_{HF}, \quad \delta\hat{g}^h_{WW} = \frac{v^2}{\Lambda^2}\left(c_{H\Box} - \frac{c_{HD}}{4}\right) \\
\kappa_{WW} &= \frac{2v^2}{\Lambda^2}c_{HW}, \quad \tilde{\kappa}_{WW} = \frac{2v^2}{\Lambda^2}c_{H\tilde{W}} \\
\delta g^Z_f &= -\frac{g' Y_f}{c_{\theta_W}}c_{WB}\frac{v^2}{\Lambda^2} - \frac{g}{c_{\theta_W}}\frac{v^2}{\Lambda^2}(|T^f_3|c^{(1)}_{HF} - T^f_3 c^{(3)}_{HF} + (1/2 - |T^f_3|)c_{Hf})c_{\theta_W} \\
&+ \frac{\delta m^2_Z}{m^2_Z}\frac{g}{2c_{\theta_W}s^2_{\theta_W}}(T_3 c^2_{\theta_W} + Y_f s^2_{\theta_W}) \\
\delta\hat{g}^h_{ZZ} &= \frac{v^2}{\Lambda^2}\left(c_{H\Box} + \frac{c_{HD}}{4}\right), \quad g^h_{Zf} = -\frac{2g}{c_{\theta_W}}\frac{v^2}{\Lambda^2}(|T^f_3|c^{(1)}_{HF} - T^f_3 c^{(3)}_{HF} + (1/2 - |T^f_3|)c_{Hf}) \\
\kappa_{ZZ} &= \frac{2v^2}{\Lambda^2}(c^2_{\theta_W}c_{HW} + s^2_{\theta_W}c_{HB} + s_{\theta_W}c_{\theta_W}c_{HWB}) \\
\tilde{\kappa}_{ZZ} &= \frac{2v^2}{\Lambda^2}(c^2_{\theta_W}c_{H\tilde{W}} + s^2_{\theta_W}c_{H\tilde{B}} + s_{\theta_W}c_{\theta_W}c_{H\tilde{W}B}), \quad \delta\hat{g}^h_{bb} = yyyc_{y_b}
\end{aligned}
$$

EFT validity

- Till now, we have dropped the $gg \to Zh$ contribution which is $\sim 15\%$ of the qq rate
- It doesn't grow with energy in presence of the anomalous couplings
- We estimate the scale of new physics for a given δg^h_{Zf}
- Example: Heavy $SU(2)_L$ triplet (singlet) vector W'^a (Z') couples to SM fermion current $\bar{f}\sigma^a\gamma_\mu f$ ($\bar{f}\gamma_\mu f$) with g_f and to the Higgs current $iH^\dagger\sigma^a \overleftrightarrow{D}_\mu H$ ($iH^\dagger \overleftrightarrow{D}_\mu H$) with g_H

$$g^h_{Zf} \sim \frac{g_H g g_f v^2}{\Lambda^2} \qquad g^h_{Zu_L,d_L} \sim \frac{g_H g^2 v^2}{2\Lambda^2}, \qquad g^h_{Zu_R,d_R} \sim \frac{g_H g g' Y_{u_R,d_R} v^2}{\Lambda^2}$$

- $\Lambda \to$ mass scale of vector and thus cut-off for low energy EFT
- Assumed g_f to be a combination of $g_B = g' Y_f$ and $g_W = g/2$ for universal case

The EFT space directions at high energies

- Five directions: g^h_{Zf} with $f = u_L, u_R, d_L, d_R$ and $g^h_{WQ} \to$ only four operators in Warsaw basis $\to g^h_{WQ} = c_\theta \frac{g^h_{Zu_L} - g^h_{Zd_L}}{\sqrt{2}}$
- Knowing proton polarisation is not possible and hence in reality there are two directions Also, upon only considering interference terms, we have

$$g^Z_{\mathbf{u}} = g^h_{Zu_L} + \frac{g^Z_{u_R}}{g^Z_{u_L}} g^h_{Zu_R}$$

$$g^Z_{\mathbf{d}} = g^h_{Zd_L} + \frac{g^Z_{d_R}}{g^Z_{d_L}} g^h_{Zd_R} \qquad g^Z_{\mathbf{p}} = g^Z_{\mathbf{u}} + \frac{\mathcal{L}_d(\hat{s})}{\mathcal{L}_u(\hat{s})} g^Z_{\mathbf{d}}$$

$$g^Z_f = g(T^f_3 - Q_f s^2_{\theta_W})/c_{\theta_W}$$

$$g^Z_{\mathbf{p}} = g^h_{Zu_L} - 0.76\, g^h_{Zd_L} - 0.45\, g^h_{Zu_R} + 0.14\, g^h_{Zd_R}$$

$$\begin{aligned} g^h_{Z\mathbf{p}} \;=\; & 2\delta g^h_{Zu_L} - 1.52\, g^h_{Zd_L} - 0.90\, g^h_{Zu_R} + 0.28\, g^h_{Zd_R} \\ & -0.14\, \delta\kappa_\gamma - 0.89\, \delta g^Z_1 \end{aligned}$$

$$g^h_{Z\mathbf{p}} \;=\; -0.14\, (\delta\kappa_\gamma - \hat{S} + Y) - 0.89\, \delta g^Z_1 - 1.3\, W$$

The four di-bosonic channels

- The four directions, *viz.*, Zh, Wh, W^+W^- and $W^\pm Z$ can be expressed (at high energies) respectively as G^0h, G^+h, G^+G^- and $G^\pm G^0$ and the Higgs field can be written as

$$\begin{pmatrix} G^+ \\ \frac{h+iG^0}{2} \end{pmatrix}$$

- These four final states are intrinsically connected
- At high energies W/Z production dominates
- With the Goldstone boson equivalence it is possible to compute amplitudes for various components of the Higgs in the unbroken phase
- Full SU(2) theory is manifest [Franceschini, Panico,Pomarol, Riva, Wulzer, 2017]

BDRS: An aside

2

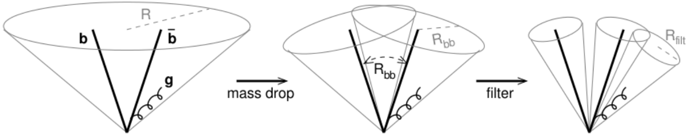

FIG. 1: The three stages of our jet analysis: starting from a hard massive jet on angular scale R, one identifies the Higgs neighbourhood within it by undoing the clustering (effectively shrinking the jet radius) until the jet splits into two subjets each with a significantly lower mass; within this region one then further reduces the radius to R_{filt} and takes the three hardest subjets, so as to filter away UE contamination while retaining hard perturbative radiation from the Higgs decay products.

Given a hard jet j, obtained with some radius R, we then use the following new iterative decomposition procedure to search for a generic boosted heavy-particle decay. It involves two dimensionless parameters, μ and y_{cut}:

1. Break the jet j into two subjets by undoing its last stage of clustering. Label the two subjets j_1, j_2 such that $m_{j_1} > m_{j_2}$.
2. If there was a significant mass drop (MD), $m_{j_1} < \mu m_j$, and the splitting is not too asymmetric, $y = \frac{\min(p_{tj_1}^2, p_{tj_2}^2)}{m_j^2} \Delta R_{j_1,j_2}^2 > y_{\text{cut}}$, then deem j to be the heavy-particle neighbourhood and exit the loop. Note that $y \simeq \min(p_{tj_1}, p_{tj_2}) / \max(p_{tj_1}, p_{tj_2})$.[1]
3. Otherwise redefine j to be equal to j_1 and go back to step 1.

The final jet j is to be considered as the candidate Higgs boson if both j_1 and j_2 have b tags. One can then identify $R_{b\bar{b}}$ with $\Delta R_{j_1 j_2}$. The effective size of jet j will thus be just sufficient to contain the QCD radiation from the

In practice the above procedure is not yet optimal for LHC at the transverse momenta of interest, $p_T \sim 200-300\,\text{GeV}$ because, from eq. (1), $R_{b\bar{b}} \gtrsim 2m_H/p_T$ is still quite large and the resulting Higgs mass peak is subject to significant degradation from the underlying event (UE), which scales as $R_{b\bar{b}}^4$ [15]. A second novel element of our analysis is to *filter* the Higgs neighbourhood. This involves resolving it on a finer angular scale, $R_{\text{filt}} < R_{b\bar{b}}$, and taking the three hardest objects (subjets) that appear — thus one captures the dominant $\mathcal{O}(\alpha_s)$ radiation from the Higgs decay, while eliminating much of the UE contamination. We find $R_{\text{filt}} = \min(0.3, R_{b\bar{b}}/2)$ to be rather effective. We also require the two hardest of the subjets to have the b tags.

ZH: Four directions in the EFT space (SILH Basis)

$$
\begin{aligned}
g^h_{Zu_Lu_L} &= \frac{g}{c_{\theta_W}}\frac{m_W^2}{\Lambda^2}(c_W + c_{HW} - c_{2W} - \frac{t^2_{\theta_W}}{3}(c_B + c_{HB} - c_{2B})) \\
g^h_{Zd_Ld_L} &= -\frac{g}{c_{\theta_W}}\frac{m_W^2}{\Lambda^2}(c_W + c_{HW} - c_{2W} + \frac{t^2_{\theta_W}}{3}(c_B + c_{HB} - c_{2B})) \\
g^h_{Zu_Ru_R} &= -\frac{4gs^2_{\theta_W}}{3c^3_{\theta_W}}\frac{m_W^2}{\Lambda^2}(c_B + c_{HB} - c_{2B}) \\
g^h_{Zd_Rd_R} &= \frac{2gs^2_{\theta_W}}{3c^3_{\theta_W}}\frac{m_W^2}{\Lambda^2}(c_B + c_{HB} - c_{2B})
\end{aligned}
$$

ZH: Four directions in the EFT space (Higgs Primaries Basis)

$$
\begin{aligned}
g^h_{Zu_Lu_L} &= 2\delta g^Z_{Zu_Lu_L} - 2\delta g^Z_1 (g^Z_f c_{2\theta_W} + eQ s_{2\theta_W}) + 2\delta\kappa_\gamma g' Y_h \frac{s_{\theta_W}}{c^2_{\theta_W}} \\
g^h_{Zd_Ld_L} &= 2\delta g^Z_{Zd_Ld_L} - 2\delta g^Z_1 (g^Z_f c_{2\theta_W} + eQ s_{2\theta_W}) + 2\delta\kappa_\gamma g' Y_h \frac{s_{\theta_W}}{c^2_{\theta_W}} \\
g^h_{Zu_Ru_R} &= 2\delta g^Z_{Zu_Ru_R} - 2\delta g^Z_1 (g^Z_f c_{2\theta_W} + eQ s_{2\theta_W}) + 2\delta\kappa_\gamma g' Y_h \frac{s_{\theta_W}}{c^2_{\theta_W}} \\
g^h_{Zd_Rd_R} &= 2\delta g^Z_{Zd_Rd_R} - 2\delta g^Z_1 (g^Z_f c_{2\theta_W} + eQ s_{2\theta_W}) + 2\delta\kappa_\gamma g' Y_h \frac{s_{\theta_W}}{c^2_{\theta_W}}
\end{aligned}
$$

[Gupta, Pomarol, Riva, 2014]

ZH: Four directions in the EFT space (Universal model Basis)

$$
\begin{aligned}
g^h_{Zu_Lu_L} &= -\frac{g}{c_{\theta_W}}\left((c^2_{\theta_W} + \frac{s^2_{\theta_W}}{3})\delta g^Z_1 + W + \frac{t^2_{\theta_W}}{3}(\hat{S} - \delta\kappa_\gamma - Y)\right) \\
g^h_{Zd_Ld_L} &= \frac{g}{c_{\theta_W}}\left((c^2_{\theta_W} - \frac{s^2_{\theta_W}}{3})\delta g^Z_1 + W - \frac{t^2_{\theta_W}}{3}(\hat{S} - \delta\kappa_\gamma - Y)\right) \\
g^h_{Zu_Ru_R} &= -\frac{4gs^2_{\theta_W}}{3c^3_{\theta_W}}(\hat{S} - \delta\kappa_\gamma + c^2_{\theta_W}\delta g^Z_1 - Y) \\
g^h_{Zd_Rd_R} &= \frac{2gs^2_{\theta_W}}{3c^3_{\theta_W}}(\hat{S} - \delta\kappa_\gamma + c^2_{\theta_W}\delta g^Z_1 - Y)
\end{aligned}
$$

[Franceschini, Panico, Pomarol, Riva, Wulzer, 2017]

The four dibosonic channels

Amplitude	High-energy primaries
$\bar{u}_L d_L \to W_L Z_L, W_L h$	$\sqrt{2} a_q^{(3)}$
$\bar{u}_L u_L \to W_L W_L$ $\bar{d}_L d_L \to Z_L h$	$a_q^{(1)} + a_q^{(3)}$
$\bar{d}_L d_L \to W_L W_L$ $\bar{u}_L u_L \to Z_L h$	$a_q^{(1)} - a_q^{(3)}$
$\bar{f}_R f_R \to W_L W_L, Z_L h$	a_f

Amplitude	High-energy primaries
$\bar{u}_L d_L \to W_L Z_L, W_L h$	$\dfrac{g^h_{Zd_L d_L} - g^h_{Zu_L u_L}}{\sqrt{2}}$
$\bar{u}_L u_L \to W_L W_L$ $\bar{d}_L d_L \to Z_L h$	$g^h_{Zd_L d_L}$
$\bar{d}_L d_L \to W_L W_L$ $\bar{u}_L u_L \to Z_L h$	$g^h_{Zu_L u_L}$
$\bar{f}_R f_R \to W_L W_L, Z_L h$	$g^h_{Zf_R f_R}$

VH and *VV* channels are entwined by symmetry and they constrain the same set of observables at High energies but may have different directions [Franceschini, Panico,Pomarol, Riva, Wulzer, 2017 & SB, Gupta, Reiness, Seth (in progress)]

Higgs-Strahlung at FCC-hh

- With a similar analysis, we obtain much stronger bounds with the 100 TeV collider

	Our 100 TeV Projection	Our 14 TeV projection	LEP Bound
$\delta g^Z_{u_L}$	± 0.0003 (± 0.0001)	± 0.002 (± 0.0007)	-0.0026 ± 0.0016
$\delta g^Z_{d_L}$	± 0.0003 (± 0.0001)	± 0.003 (± 0.001)	0.0023 ± 0.001
$\delta g^Z_{u_R}$	± 0.0005 (± 0.0002)	± 0.005 (± 0.001)	-0.0036 ± 0.0035
$\delta g^Z_{d_R}$	± 0.0015 (± 0.0006)	± 0.016 (± 0.005)	0.0016 ± 0.0052
δg^Z_1	± 0.0005 (± 0.0002)	± 0.005 (± 0.001)	$0.009^{+0.043}_{-0.042}$
$\delta \kappa_\gamma$	± 0.0035 (± 0.0015)	± 0.032 (± 0.009)	$0.016^{+0.085}_{-0.096}$
$\hat{S}$	± 0.0035 (± 0.0015)	± 0.032 (± 0.009)	0.0004 ± 0.0007
W	± 0.0004 (± 0.0002)	± 0.003 (± 0.001)	0.0000 ± 0.0006
Y	± 0.0035 (± 0.0015)	± 0.032 (± 0.009)	0.0003 ± 0.0006

[SB, Englert, Gupta, Spannowsky (in progress)]